DISSIPATIVE ENERGY AND STORED ELASTIC ENERGY DURING LIQUEFACTION PROCESS

Yoshimi OGAWA[1], Kaoru KUSANO[2] And Hiroshi ABE[3]

SUMMARY

A calculating method is proposed to evaluate the dissipative energy and the stored elastic energy of a soil element during a liquefaction test. The dissipative energy is determined as continuous values and the stored elastic energy is calculated as the difference between the shear work and the dissipative energy. To study the relationship among the excess pore water pressure, the dissipative energy and the stored elastic energy, several series of liquefaction tests were done. Four types of sandy soil, disturbed and undisturbed samples, were used as the test materials and various amplitudes of sinusoidal waves and earthquake motions were loaded as shear stress.

There is a characteristic relationship between the dissipative energy and the observed excess pore water pressure buildup in each step of shear stress. The square root of the dissipative energy is proportional to the increase of observed excess pore water pressure. This means that the energy owing to the negative dilatancy of sand is proportional to the dissipative energy. The stored elastic energy is approximately proportional to the temporary decrease of excess pore water pressure with large shear strain.

INTRODUCTION

It is known that the dissipative energy is closely related to the pore water pressure development during liquefaction process. Towhata and Ishihara [Towhata and Ishihara (1985)] carried out several kinds of cyclic loading tests, and calculated the dissipative energy as the shear work. They found that there is a unique relationship between the shear work and the pore water pressure buildup, and this relation is independent of the shear-stress history. Similar studies were accomplished by Sakai and Ochiai [Sakai and Ochiai (1986)], and by Taji et al. [Taji et al. (1993)]. Nakano and Saito [Nakano and Saito (1993)] measured the dissipative energy from area of hysteresis loops, and derived the independence of shear-stress amplitude on the relation between the dissipative energy and the development of pore pressure.

In these previous studies, the dissipated energy is not obtained as a continuous function but as discrete quantities. The shear work is theoretically equivalent to the dissipative energy in elasto-plastic body when the incremental shear work is calculated by a half cycle, ranging in stress from 0 to 0 in each integral step. The area of hysteresis loop can be measured by each half cycle, too. But the stress-strain relations of soil element during liquefaction process do not show the relation of elasto-plastic body and their hysteresis loops do not close in each cycle, correctly.

---

[1]   Institute of Civil Engineering of Tokyo Metropolitan Government, Japan Email:Ogawa.Yoshimi@iri.metro.tokyo.jp
[2]   Institute of Civil Engineering of Tokyo Metropolitan Government, Japan Email:Ogawa.Yoshimi@iri.metro.tokyo.jp
[3]   Department of Civil Engineering, Gunma College of Technology, Japan Email:abe@cvl.gunma-ct.ac.jp

The authors have proposed the calculating method to determine the dissipative energy as a continuous function during sinusoidal loading [Ogawa et al. (1995)]. This method bases its concept on the mechanical model of elasto-plastic body proposed by Iwan [(Iwan 1966)]. The stored potential energy is estimated as the difference in energy between the shear work and the dissipative energy.

In this paper, the authors propose the improved method to calculate the dissipative energy of irregular loading such as the time history of shear stress during an earthquake. The method was applied to the results of several liquefaction element tests such as various amplitudes of sinusoidal shear stress tests and irregular shear stress tests simulated earthquake stress motions.

ANALYTICAL METHOD

Dissipative Energy of curvilinear relations

Most soils have curvilinear stress-strain relationships while excess pore water pressure is not accumulated. The gradient of the skeleton curve is decrease constantly according as the strain as illustrated in **Figure 1**. In this figure, we denote a strain amplitude γ and infinite increment and decrement $\pm \Delta\gamma$ across γ. The shear stress τ increases as $\tau(\gamma-\Delta\gamma)$, $\tau(\gamma)$ and $\tau(\gamma+\Delta\gamma)$ according to increase in shear strain as $\gamma-\Delta\gamma$, γ and $\gamma+\Delta\gamma$, respectively. Now we suppose the shear stress increases linearly, and denote the shear rigidity as G ranging from $\gamma-\Delta\gamma$ to γ and $G-\Delta G$ ranging from γ to $\gamma+\Delta\gamma$, respectively

The decrease in the shear rigidity is closely related to the dissipative energy during curvilinear relations. It is easy to comprehend the relation of the shear rigidity decrement ΔG and the dissipative energy by the mechanical model of elasto-plastic body proposed by Iwan(1966). This model composed of simple linear springs and Coulomb friction elements arranged as shown in **Figure 2**. The friction elements remain locked until the spring force on them exceeds, then dislocate. The decrease in shear rigidity means the beginning of dislocation of a certain friction element. The dissipative energy generates by the dislocation of this friction element. The frictional force of the element is equivalent to the spring force connected to the element, and the spring coefficient is the same as the shear rigidity decrement ΔG. The friction force of the sliding element $\Delta\tau$ is defined as follows.

$$\Delta\tau = \Delta G \cdot \gamma \qquad (1)$$

When the shear strain increases from γ to Γ, the dissipative energy of the friction element Δe is the same as the shear work of the frictional force $\Delta\tau$. And the dissipative energy is derived from multiplying the friction $\Delta\tau$ by the strain increment $\Gamma-\gamma$ as the following equation:

$$\Delta e = \Delta\tau \cdot (\Gamma - \gamma) \qquad (2)$$

The total dissipative energy of the skeleton curve process e_1 is determined by the integration from origin to Γ of equation (2) as follows:

$$e_1 = \int_0^\Gamma -\frac{d}{d\gamma}G(\gamma) \cdot \gamma \cdot (\Gamma - \gamma) \cdot d\gamma \qquad (3)$$

Figure 1: Decrease in shear rigidity and the dissipative energy of skeleton curve
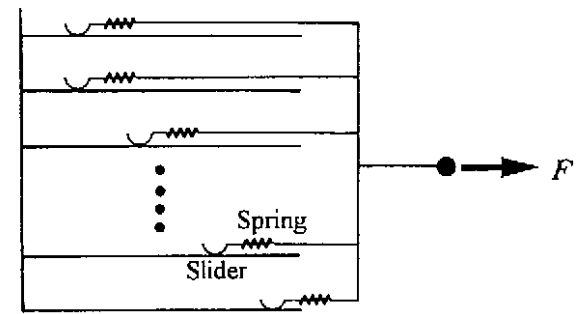
Figure 2:Mechanical model of elasto-plastic body proposed by Iwan(1966)

The energy dissipation during hysteretic curves is determined in a similar way to the skeleton curve. But the equation must be modified to account of the fact that the shape of a hysteretic curve is different from the shape

of a skeleton curve. According to Masing's law [Ohsaki (1980)], the shape of the hysteretic curve is multiplying the shape of the skeleton curve by 2. This rule is explained from Iwan's mechanical model that the completely expanded (or contracted) spring is applied reverse force then contracting (or expanding) until the spring force reaches the friction of Coulomb element. It means that the strain value for estimating frictional force is double-counted in equation (1). Therefore the shear strain γ must be $\gamma/2$ in the hysteretic curve process.

If shear strain reaches the maximum strain value of past stress-strain relations, the hysteretic curve meets the skeleton curve. Shear strain exceeds the maximum past strain γ_{max}, the hysteretic curve follows along the skeleton curve and the shape of the hysteretic curve is the same as the skeleton curve. Consequently, the shear strain of equation (1) must be reset as γ. To summarize the relations mentioned above, the dissipative energy e_i of the hysteresis loops are given as the following equations.

$$e_i = \int_{\gamma_0}^{\Gamma} -\frac{d}{d\gamma}G(\gamma) \cdot \frac{\gamma - \gamma_0}{2} \cdot (\Gamma - \gamma) \cdot d\gamma \qquad \text{for } |\gamma| \leq \gamma_{max}$$

$$e_i = \int_{\gamma_0}^{\gamma_{max}} -\frac{d}{d\gamma}G(\gamma) \cdot \frac{\gamma - \gamma_0}{2} \cdot (\Gamma - \gamma) \cdot d\gamma + \int_{\gamma_{max}}^{\Gamma} -\frac{d}{d\gamma}G(\gamma) \cdot \gamma \cdot (\Gamma - \gamma) \cdot d\gamma \qquad (4)$$

$$\text{for } |\gamma| > \gamma_{max}$$

Where, γ_0 is the strain at the turning point of the hysteretic curve and selection of the unloading point or the reloading point is according as the unloading or reloading curve. To change equation (4) into a partial integral, it is proved that the dissipative energy of one cycle of a hysteresis loop is same as the area enclosed with the hysteresis loop.

The total dissipative energy E_L is obtained by sum of e_i for the skeleton curve and the unload and reload curves of hysteresis loops as follows:

$$E_L = \sum_i e_i \qquad (5)$$

Dissipative energy of observed stress-strain relations during liquefaction process

The stress-strain relations during liquefaction process show "banana loop" shapes and do not agree with the relations of curvilinear process. This phenomenon is caused by the pore water pressure buildup. Increase or decrease in the shear stress is according as decrease or increase in the excess pore water pressure.

To evaluate the dissipative energy of observed stress-strain relations, use is made of the following assumption: The shear stress τ is proportional to the effective confining stress σ'.

It is well known that the shear stress is proportional to $(\sigma')^m$, precisely (Silver and Seed, 1971). The multiplier m is less than 1.0 and approaches 1.0 as the strain amplitude increases. Consequently, the assumption mentioned above gives approximate results and causes errors within a small strain range, but these errors are negligible in a large strain range. Almost all part of liquefaction process progresses in the large strain range, therefore the errors of the assumption are supposed to be negligible.

According to the assumption, equation (1) is changed into difference equation and (3) is modified as follows:

$$\Delta\tau' = \left[\frac{\tau(\gamma)/\sigma'(\gamma) - \tau(\gamma-\Delta\gamma)/\sigma'(\gamma-\Delta\gamma)}{\Delta\gamma} - \frac{\tau(\gamma+\Delta\gamma)/\sigma'(\gamma+\Delta\gamma) - \tau(\gamma)/\sigma'(\gamma)}{\Delta\gamma} \right] \cdot \gamma \qquad (6)$$

$$e_i' = \int_0^{\Gamma} \Delta\tau' \cdot \sigma'(\gamma) \cdot d\gamma \qquad (7)$$

Where $\Delta\tau'$ and e_i' are the friction force and the total dissipative energy in effective stress condition, respectively. To calculate equation (6) and (7) simultaneously, the increment of dissipative energy $\Delta E'_{i,m}$ in effective stress condition during the skeleton curve and the hysteresis loops are derived from equation (4) and (7).

$$\Delta E_{1,m}' = \left[\left(\frac{\tau(m-1)}{\sigma'(m-1)} \right) \cdot (\gamma(m) - \gamma(m-1)) - \left(\frac{\tau(m)}{\sigma'(m)} - \frac{\tau(m-1)}{\sigma'(m-1)} \right) \cdot \gamma(m-1) \right] \cdot \frac{\sigma'(m-1) + \sigma'(m)}{2}$$

for skeletoncurve

$$\Delta E_{i,m}' = \frac{1}{2} \left[\left(\frac{\tau(m-1)}{\sigma'(m-1)} - \frac{\tau(0)}{\sigma'(0)} \right) \cdot (\gamma(m) - \gamma(m-1)) - \left(\frac{\tau(m)}{\sigma'(m)} - \frac{\tau(m-1)}{\sigma'(m-1)} \right) \cdot (\gamma(m-1) - \gamma(0)) \right] \cdot \frac{\sigma'(m-1) + \sigma'(m)}{2}$$

for hysteresisloops and $|\gamma| \le \gamma_{\max}$

$$\Delta E_{i,m}' = \left[\frac{1}{2} \left(2 \frac{\tau(m-1)}{\sigma'(m-1)} - \frac{\tau(0)}{\sigma'(0)} - \frac{\tau(k)}{\sigma'(k)} \right) \cdot (\gamma(m) - \gamma(m-1)) - \left(\frac{\tau(m)}{\sigma'(m)} - \frac{\tau(m-1)}{\sigma'(m-1)} \right) \cdot \gamma(m-1) + \right. \tag{8}$$

$$\left. \frac{\tau(k+1)/\sigma'(k+1) - \tau(k-1)/\sigma'(k-1)}{\gamma(k) - \gamma(k-1)} \cdot \frac{\gamma(k) + \gamma(0)}{2} (\gamma(m) - \gamma(m-1)) \right] \cdot \frac{\sigma'(m-1) + \sigma'(m)}{2}$$

for hysteresisloops and $|\gamma| \succ \gamma_{\max}$

Where i denotes the number of half cycle, m the number of incremental step and k the number of the first point where the absolute strain exceeds the maximum strain of past loops. $\tau(0)$, $\gamma(0)$ and $\sigma'(0)$ are shear stress, strain and effective confining stress at the turning or the reloading point, respectively. The total dissipative energy E_L' is given by equation (9).

$$E_L' = \sum_i \sum_m \Delta E_{i,m}' \tag{9}$$

The stored potential energy E_P' is calculated as the difference in energy between the shear work W and the dissipative energy E_L' as follows:

$$E_P' = W - E_L' \tag{10}$$

LIQUEFACTION ELEMENT TEST DATA

The liquefaction element test data used for this analysis was carried out under the following conditions: a shear apparatus was a stress controlled triaxial torsion shear apparatus; a soil specimen was a hollow cylindrical shape, 7 cm high, with an inner and outer diameter of 3 and 7 cm, respectively. The disturbed test specimens are composed of Toyoura sand and compacted as 50 % and 80 % of relative density, respectively. The materials of undisturbed test are silty fine sand and sandy silt. These specimens were sampled at Nishi-Mizue on Koto word in Tokyo. The silty fine sand specimens were sampled from 3.0m to 4.1m depths and N-value of the standard penetration test is about 3. Contents of sand, silt and clay are 75.0%, 17.0% and 8.0%, respectively. Mean particle size D_{50} is 0.1622mm. The sandy silt specimens were sampled from 5.2m to 6.05m depths and N-value is 3. Contents of sand, silt and clay are 28.1%, 53.9% and 18.0%, respectively. Mean particle size D_{50} is 0.0418mm.

Table1: Void ratio, relative density and liquefaction strength of the test specimens

Soil Type	Toyoura Sand (Dr=50%)				Toyoura Sand (Dr=80%)				Silty Fine Sand				Sandy Silt			
Sampling	Disturbed				Disturbed				Undisturbed				Undisturbed			
Specimen No.	TD1	TD2	TD3	TD4	TD5	TD6	TD7	TD8	SD1	SD2	SD3	SD4	CD1	CD2	CD3	CD4
Void Ratio	0.779	0.784	0.777	0.779	0.679	0.686	0.681	0.685	0.904	0.943	0.903	0.942	1.073	1.361	1.223	0.990
Relative Density (%)	54.8	53.3	55.3	54.8	83.6	81.5	83.0	81.8	69.5	62.9	69.7	63.1	-	-	-	-
Cyclic shear stress (kPa)	19.8	15.8	14.4	26.9	26.4	37.5	55.1	23.9	31.8	26.6	21.0	52.1	35.7	30.3	26.4	41.7
DA 1.5% (No. of Cycles)	2.9	13.6	44.0	0.3	5.5	0.8	0.4	17.6	1.0	2.5	14.5	0.2	0.5	0.9	4.2	0.2
DA 3.0% (No. of Cycles)	3.2	13.8	44.6	0.6	7.8	1.7	0.8	21.3	2.2	4.5	20.1	0.4	0.9	3.4	10.9	0.5
DA 7.5% (No. of Cycles)	3.7	14.4	45.3	1.4	18.3	4.6	2.9	35.1	5.7	8.7	29.8	0.9	2.9	9.7	22.0	1.4
DA 15.0% (No. of Cycles)	4.4	15.0	46.4	1.9	54.7	14.4	11.1	.	12.2	14.7	41.0	2.4	6.1	16.9	32.0	2.7
95% of Pore Pressure ratio	3.6	13.9	44.5	1.0	8.5	2.7	2.0	20.8	6.1	8.0	25.9	1.8	.	-	-	-

Notes: Values of void ratio and relative density were observed after consolidation. Values of 95% of pore water pressure ratio are number of cycles.

All specimens were isotropically consolidated under a confining pressure of 98 kPa and back pressure of 196 kPa were applied then sinusoidal shear stress of various amplitudes were applied in cycle of 0.1 Hz under

Table 2: Experimental conditions of irregular loading tests

Soil Type	Toyoura Sand (Dr=80%)		Silty Fine Sand		Sandy Silt	
Sampling	Disturbed		Undisturbed		Undisturbed	
Specimen number	Td9	Td10	Sd5	Sd6	Cd5	Cd6
Input earthquake motion	Kaihoku br.	Kobe obs.	Miyako port	Kobe obs.	Miyako port	Kobe obs.
Void Ratio	0.679	0.681	0.890	0.912	1.482	1.393
Relative Density (%)	83.6	83.0	72.8	68.2	-	-
Maximum shear stress (kPa)	34.3	56.8	37.6	46.8	35.2	40.4
Maximum shear strain (%)	0.86	2.06	2.47	2.65	1.81	3.37
Maximum Pore Pressure ratio	0.91	0.99	0.95	0.96	0.69	0.67

undrained condition. Skenpton's B-value of more than 0.95 was obtained in all the specimens. Amplitudes of sinusoidal shear stress and liquefaction test results are shown in table 1.

The irregular loading tests were experimented with the Toyoura sand (Dr=80%), the silty fine sand and the sandy silt specimens. Test conditions are same as the sinusoidal shear tests. To simulate the time histories of shear stress during earthquakes, the observed acceleration motions were modified by multiplication factors. The acceleration motions used were following three seismograms: the 1983 Nihonkai-chubu earthquake observed at Kaihoku Bridge by Public Works Research Institute, Ministry of Construction, the same earthquake observed at Miyako Port by Port and Harbour Research Institute, Ministory of Transport, the 1995 Hyogoken-nambu earthquake observed at Kobe ocean meteorological observatory by Japan Meteorological Agency. The experimental conditions are shown in table 2.

ANALYTICAL RESULTS

The dissipative energy and excess pore water pressure during sinusoidal loading

The dissipative energy is calculated until the excess pore water pressure exceeds 95% of the initial effective confining stress. **Figure 3** shows relations between the dissipative energy and the excess pore water pressures thus obtained from a series of Toyoura sand (Dr=50%) tests. Although the amplitudes of cyclic shear stress were different in each of the tests, all the envelopes of peaks in each curve are similar in shapes. The peaks of the dissipative energy approximately correspond to the shear work evaluated within every half cycle. Therefore, the results of previous studies that the pore water pressures are uniquely correlated with the shear work of every half cycle are observed in this study.

The relationships between the square root of dissipative energy and the excess pore water pressures are illustrated in **Figure 4**. All the envelopes of peaks in each curve are approximately linear and these gradients are almost same each other ranging in the pore pressure to 70kPa. The stored elastic energy and the excess pore water pressures in calculating steps are shown in **Figure 5** (Td1) and **Figure 6** (Td2). The stored elastic energy increases vigorously ranging in the pore pressure from 70kPa, and the decrease of pore water pressures seem to be proportional to the stored elastic energy developments.

Figure 7 shows relations between the square root of dissipative energy and pore pressures obtained from Toyoura sand (Dr=80%) tests. All the envelopes of peaks in each curve are approximately similar but linear relations disappear ranging in the pore pressure from 40kPa. Corresponding to these, the stored elastic energy is
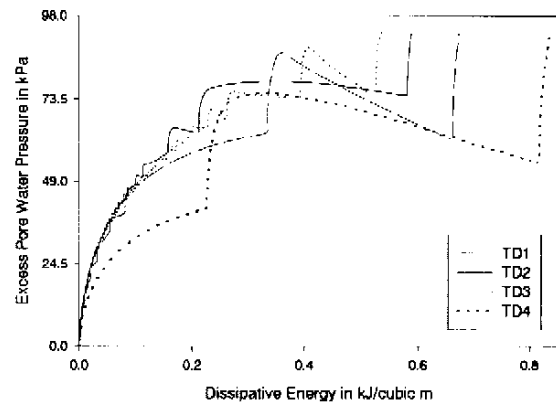
Figure 3: Relations between dissipative energy and excess pore water pressures of Toyoura sand (Dr=50%)
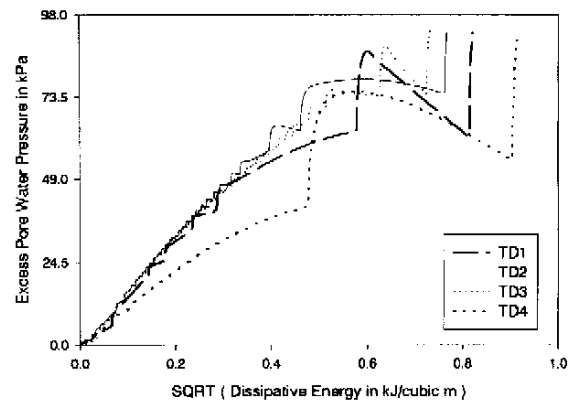
Figure 4: Relations between square root of dissipative energy and excess pore water pressures of Toyoura sand (Dr=50%)
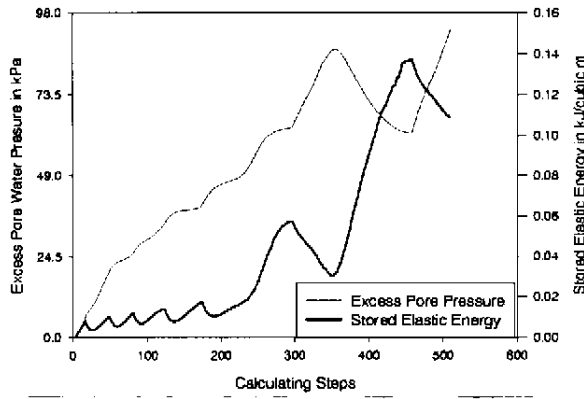
Figure 5: Stored elastic energy and pore pressures of Toyoura sand (Dr=50%, Td1)
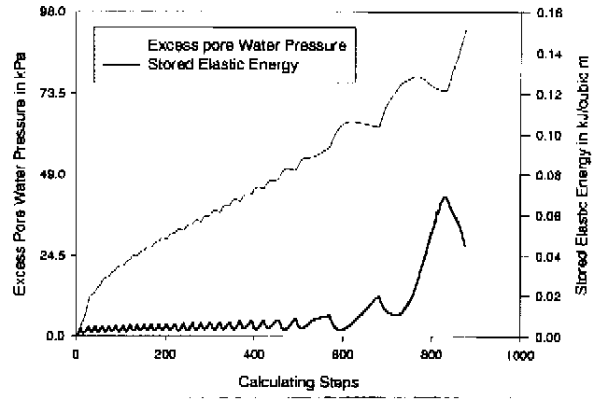
Figure 6: Stored elastic energy and pore pressures of Toyoura sand (Dr=50%, Td2)
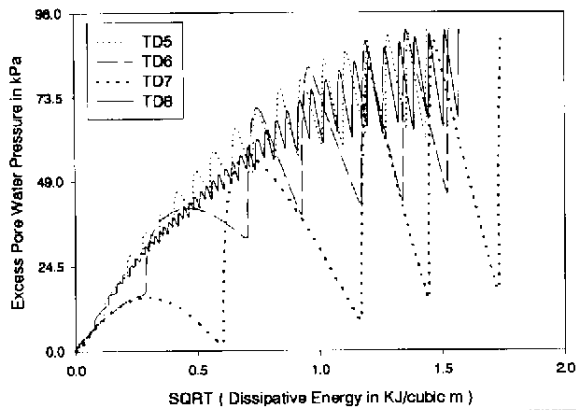
Figure 7: Relations between square root of dissipative energy and excess pore water pressures of Toyoura sand (Dr=80%)
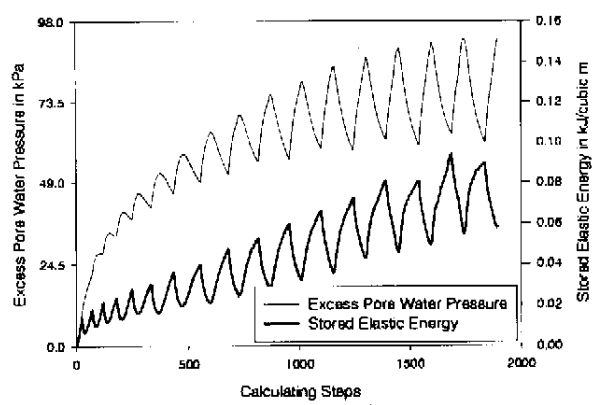
Figure 8: Stored elastic energy and pore pressures of Toyoura sand (Dr=80%, Td5)
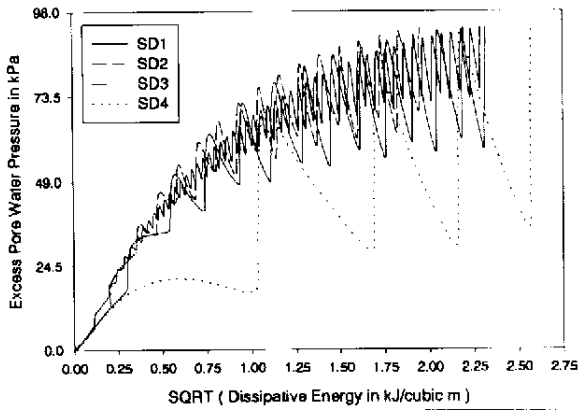
Figure 9: Relations between square root of dissipative energy and excess pore water pressures of silty fine sand
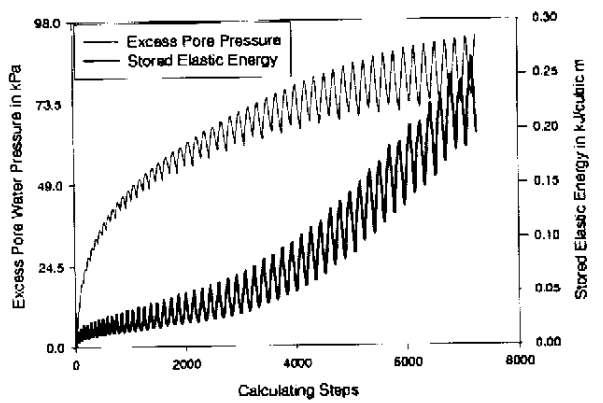
Figure 10: Stored elastic energy and pore pressures of sikty fine sand (Sd3)

increasing within early calculating steps as shown in **Figure 8**.

The relationships between the square root of dissipative energy and the pore pressures of undisturbed silty fine sand and sandy silt are shown in **Figure 9** and **Figure 11**, respectively. There are little difference among the envelope curves but the unique correlation between the envelope curves and pore water pressures are observed. The linear relations between the envelope curves and pore pressures are recognized ranging pore pressure to 40 kPa, too. The stored elastic energy and pore pressures of silty fine sand and sandy silt are illustrated in **Figure 10** and **Figure 12**. The elastic energy of both soils increases within early calculating steps.
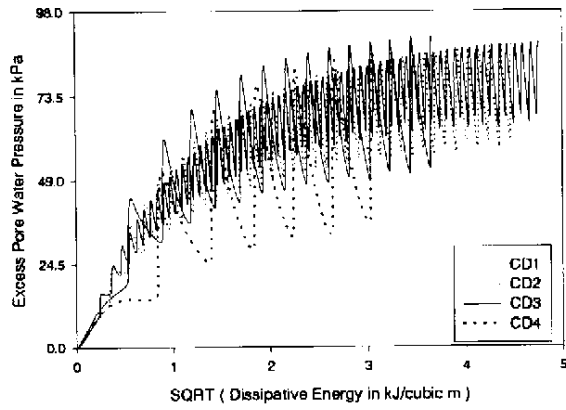
Figure 11: Relations between square root of dissipative energy and excess pore water pressures of sandy silt
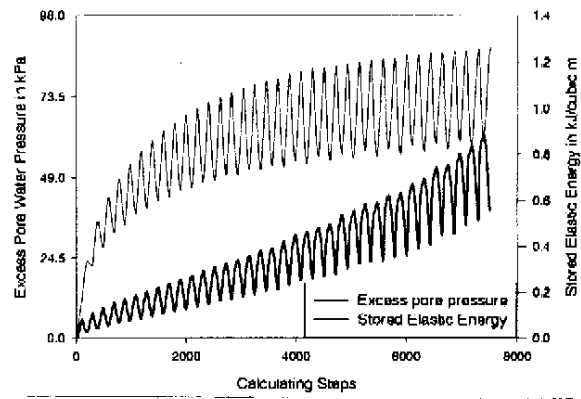
Figure 12: Stored elastic energy and pore pressures of sandy silt (Cd2)
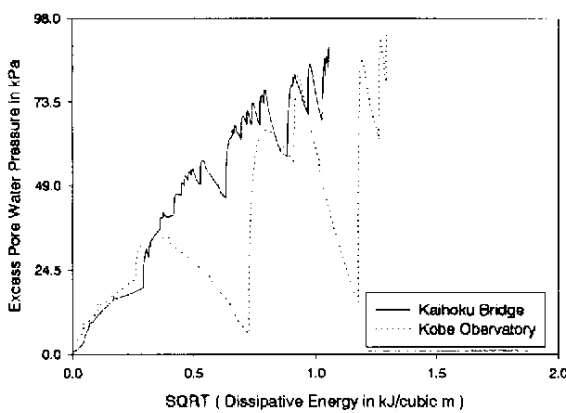
Figure 13: Relations between square root of dissipative energy and pore pressures of Toyoura dense sand (Dr=80%), irregular
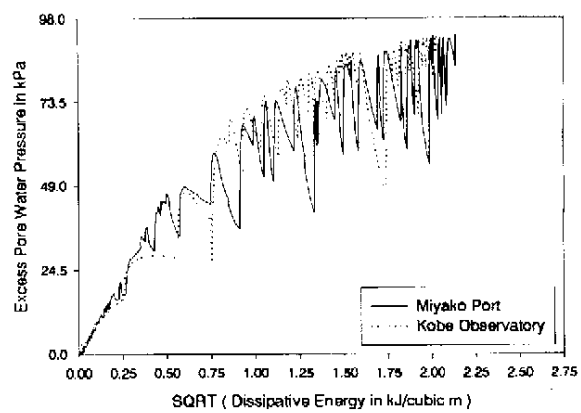
Figure 14: Relations between square root of dissipative energy and pore pressures of silty fine sand, irregular loading
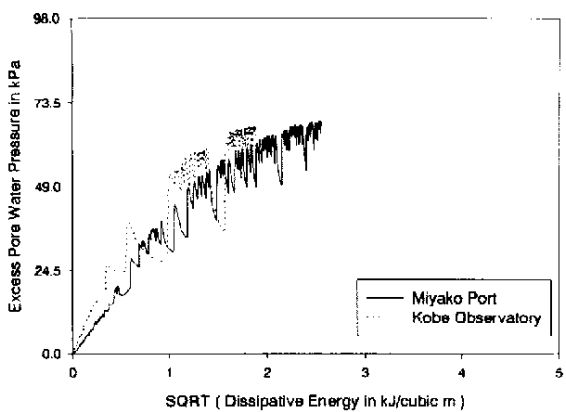
Figure 15: Relations between square root of dissipative energy and pore pressures of sandy silt, irregular loading
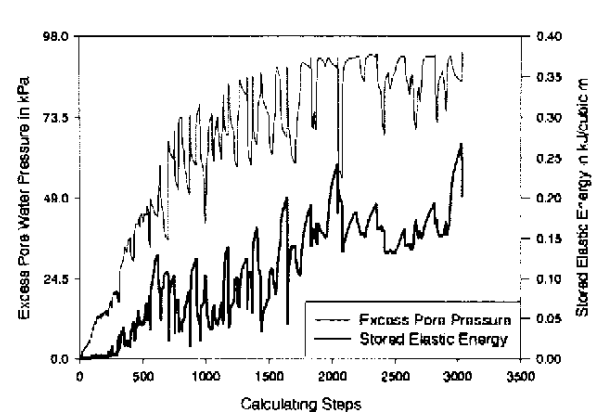
Figure 16: Stored elastic energy and pore pressures of silty fine sand, irregular loading

The dissipative energy and excess pore water pressure during irregular loading

The calculations of irregular loading were made for Toyoura dense sand (**Figure 13**), silty fine sand (**Figure 14**) and sandy silt (**Figure 15**). Each relation between the square root of dissipative energy and the pore pressures is approximately agrees with the sinusoidal ones except the calculation of sandy silt loaded with Miyako Port motion. The linear relations between the envelope curves and pore pressures are also observed. **Figure 16** shows

the stored elastic energy of silty fine sand loaded with Miyako Port motion. Vigorous increases and decreases of pore pressure correspond to the decreases and increases of stored elastic energy. The elastic energy level agrees with that of sinusoidal loading results in **Figure 10**.

CONCLUSIONS

The calculating method was proposed to evaluate the dissipative energy and the stored elastic energy of a soil element during a liquefaction test. The dissipative energy is determined as continuous values and the stored elastic energy is calculated as the difference between the shear work and the dissipative energy. The method was applied to the results of several liquefaction element tests such as various amplitudes of sinusoidal shear stress tests and irregular shear stress tests simulated earthquake stress motions.

A unique correlation between the dissipative energy and the pore water pressure developments is observed. This correlation is independent of amplitudes of sinusoidal shear stress. The pore pressure buildup to 95% of the initial effective confining stress necessitates 0.658 kJ/m^3 average dissipative energy for Toyoura loose sand, 2.48 kJ/m^3 for Toyoura dense sand, 5.26kJ/m^3 for silty fine sand and 16.4 kJ/m^3 for sandy silt. It is recognized that easily liquefiable soil requires low dissipative energy within test materials.

There are linear relations between the peaks of pore pressures and the square root of dissipative energy at each peak. These relations are observed ranging in the pore pressure to 70kPa in Toyoura loose sand and ranging to 40 kPa in other sands. The gradients of linear relations are proportional to liquefaction strength. The fact that the pore pressure developments correlate to the square root of dissipative energy means the energy owing to the negative dilatancy of sand is proportional to the dissipative energy.

In the calculations of irregular loading, each relation between the square root of dissipative energy and the pore pressures is approximately agrees with the sinusoidal ones except the calculation of sandy silt loaded with Miyako Port motion.

The stored elastic energy develops at almost the same time that the excess pore water pressures decreases temporary. The stored elastic energy values are approximately proportional to the temporary decreases of excess pore water pressure with large shear strain.

REFERENCES

Iwan, W. D. (1966),"A distributed-element model for hysteresis and its steady-state dynamic response, Journal of Applied Mechanics, pp893-900.

Nakano, H. and Saito, E. (1993), "Relation between excess pore water pressure and energy during liquefaction", Proceedings of the 48th Annual Conference of JSCE, 3, pp486-487. *in Japanese*.

Ogawa, Y.,Abe, H. and Yoshitsugu, S. (1995),"Energy loss and stored elastic energy during liquefaction process", First International Conference on Earthquake Geotechnical Engineering, 2, pp957-962.

Ohsaki, I. (1980),"Some notes on Masing's low and non-linear response of soil deposites, Journal of the Faculty of Engineering, the University of Tokyo, pp513-536.

Sakai, A. and Ochiai, H. (1986),"A liquefaction analysis of saturated sand ground based on shear works", Proceedings of JSCE, 370/3, 5, pp75-83, *in Japanese with English abstract*.

Taji, Y., Sugano, T., Yanagisawa, E. and Yamamoto, H. (1993),"Characteristics of liquefaction phenomena considering shear work", The 28th Japan National Conference on Soil Mechanics and Foundation Engineering, pp967-968, *in Japanese*.

Towhata, I. and Ishihara K. (1985),"Shear work and pore water pressure in undrained shear", Soils and Foundations, 25, 3, pp73-84.